

Deakin Research Online

This is the published version:

Weiss, Matthias, Rolfe, Bernard, Yang, Chunhui, De Souza, Tim and Hodgson, Peter 2011, Review of approximate analyses of sheet forming processes, in *NUMISHEET 2011 : American Institute of Physics Conference Proceedings*, American Institute of Physics, [Seoul, Korea], pp. 986-996.

Available from Deakin Research Online:

<http://hdl.handle.net/10536/DRO/DU:30042259>

Copyright (2011) American Institute of Physics. This article may be downloaded for personal use only. Any other use requires prior permission of the author and the American Institute of Physics.

Copyright : 2011, American Institute of Physics

Review of Approximate Analyses of Sheet Forming Processes

Matthias Weiss^b, Bernard Rolfe^{a*}, Chunhui Yang^a, Tim de Souza^b, Peter Hodgson^b

^a School of Engineering, Deakin University, Waurn Ponds, Victoria, Australia. 3217

^b Institute for Technology Research and Innovation, Deakin University, Waurn Ponds, Victoria, Australia. 3217
*corresponding author: bernard.rolfe@deakin.edu.au

Abstract. Approximate models are often used for the following purposes:

- in on-line control systems of metal forming processes where calculation speed is critical;
- to obtain quick, quantitative information on the magnitude of the main variables in the early stages of process design;
- to illustrate the role of the major variables in the process;
- as an initial check on numerical modelling; and
- as a basis for quick calculations on processes in teaching and training packages.

The models often share many similarities; for example, an arbitrary geometric assumption of deformation giving a simplified strain distribution, simple material property descriptions - such as an elastic, perfectly plastic law - and mathematical short cuts such as a linear approximation of a polynomial expression. In many cases, the output differs significantly from experiment and performance or efficiency factors are developed by experience to tune the models. In recent years, analytical models have been widely used at Deakin University in the design of experiments and equipment and as a pre-cursor to more detailed numerical analyses. Examples that are reviewed in this paper include deformation of sandwich material having a weak, elastic core, load prediction in deep drawing, bending of strip (particularly of ageing steel where kinking may occur), process analysis of low-pressure hydroforming of tubing, analysis of the rejection rates in stamping, and the determination of constitutive models by an inverse method applied to bending tests.

Keywords: Stamping, hydroforming, roll forming, analytical modelling, laminates

PACS: 81.05.Bx, 83.50.Uv, 81.40.Lm, 81.20.Hy

INTRODUCTION

Metal forming studies have followed several traditional approaches; one, the mathematical, continuum mechanics style, another using extensive numerical modelling, mainly finite element techniques and thirdly the method that can be described as engineering plasticity. The latter was pioneered by, to name just a few, Johnson and Mellor, Marciniak, Fukui, Sachs, Popov and Backofen. This follows more the approach of strength of materials for elastic materials in that it uses approximations and simplifying assumptions to reduce the problem to formulae that allow rapid calculation. The object of engineering plasticity has been not only to provide numbers for process design, but also to identify the governing variables so that students can obtain in their minds an understanding of the limits of a metal forming operation.

Two very clever, but at the same time essentially simple examples of models that have been extensively used over the years can be mentioned. The Bland and Ford approximation [1] for the roll force in slab rolling is;

$$F = Y\sqrt{R\Delta h} \quad (1)$$

where F is the roll force per unit width, R , the roll radius and, Δh , the reduction. The analysis is based on the assumption that the stress on the deformation length, $\sqrt{R\Delta h}$, is the yield stress, Y . In the early control algorithms for

automatic gauge control in strip mills, a tuned version of this equation was used and in teaching this is a useful starting point as it shows how roll radius affects the roll force.

Another model still widely used for predicting springback in sheet metal forming is the Gardiner equation [2];

$$\Delta\theta = \frac{Y R}{E t} \theta \quad (2)$$

where, $\Delta\theta$, is the springback, E , is Youngs modulus, R , the bend radius and, t , the sheet thickness. The assumption is that the sheet is fully plastic before unloading and that there is no axial tension; the equation presented is also simplified mathematically.

At Deakin University, closed form approximations have been used in the initial stages of study of a number of metal forming studies and these are reviewed briefly here. It should perhaps be mentioned that there is a recommended approach to all these problems that follows the order given below:

- Geometry: describe the deformation of the material in a simple and approximate form which will lead to defining the strain distribution.
- Equilibrium: write down the equilibrium equations that apply without, as yet, specifying the material behaviour.
- Material behaviour: describe material behaviour by a simple constitutive law.

In this review, the different processes studied are presented briefly. In all cases, the above approach was used and, for brevity, only the simplifying assumptions are described.

DEEP DRAWING

Many analytical models have been used for deep drawing of a circular cup [3]; for a rigid, perfectly plastic material a typical model can be summarized in the equation,

$$F = 2\pi R_i \left[1.13\bar{\sigma}t_0 \ln\left(\frac{r_0}{R_i}\right) + \frac{\mu B}{\pi t_0} \right] \exp(\mu\theta) \sin(\theta) \quad (3)$$

where the variables are illustrated in Figure 1 and, r_0 , and, R_i , are the outer blank radius and cup radius respectively. The cup wall angle, θ , can be found from trigonometry.

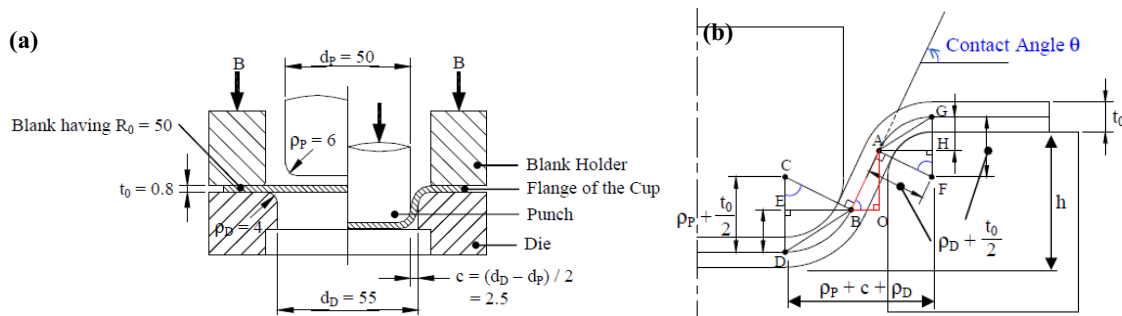


FIGURE 1. (a) Schematic diagram of the deep drawing of a cylindrical cup (dimensions in millimeters) and (b) Geometry of deep-drawn cup for determination of the contact angle θ .

This model was extended to include strain hardening and the details are given in Ref. 4. Constant thickness deformation was assumed to exist throughout and at any instant in the process, the average yield stress, $\bar{\sigma}_{av}$, was taken as the effective stress for an element on the flange at a radius that divided the flange into two equal areas. The effective strain for this radius can be readily determined from the initial and current blank dimensions. To test this model, commercial quality cold rolled sheet steel was deep drawn, and the experimental and theoretical punch displacement curves are shown in Figure 2. This also shows the results of finite element analysis of the process using Abaqus/Standard; the results using two models, shell elements (SAX1) and solid elements (CAX4R), are also shown in this diagram.

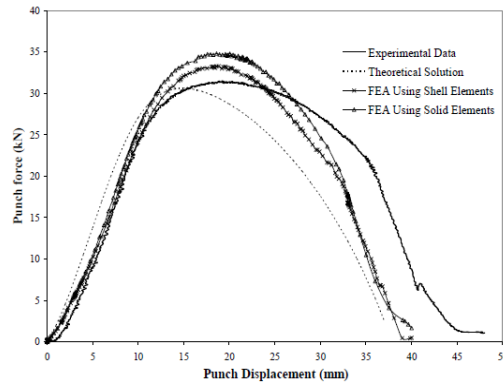


FIGURE 2. Punch displacement-force diagram.

The closed form solution gives slightly better prediction of the maximum drawing force than the finite element analyses; all the models under-estimate the punch force in the final stages of the process. The advantage of this approximate model [5] is that the effect of friction, strain hardening and tool geometry on the outcome of the drawing operation can be assessed quickly and this is valuable both in process design and in teaching.

ASSESSMENT OF REJECTION RATES

The inherent variability of the incoming sheet and the die conditions in a stamping operation can influence the quality of the final product and cause excessive rejects. A single finite element simulation is successful at predicting the forming behaviour and springback of a stamping process; however, it lacks the ability to assess the influence of the true stochastic nature of the process. In this work [6], a probabilistic analytical model has been developed to investigate the effect of variation in material and process conditions on the shape stability or springback for a simple stretch forming process. The stamping process is simplified to the two-dimensional stretching of a thin sheet over a gently curved form block, as shown in Figure 3, the applied tension in the sidewall is used to simulate various process operating windows. The rejection criterion was based on an arbitrarily assigned acceptable limit of springback which was measured by the change in the radius of curvature; a simple model [3] gives the change in curvature as:

$$\frac{\Delta(1/\rho)}{(1/\rho)} = -\frac{|d\sigma_1/d\varepsilon_1|_{\varepsilon_{1a}}}{E} \quad (4)$$

where $|d\sigma_1/d\varepsilon_1|_{\varepsilon_{1a}}$ is the plastic modulus of the material for the mid-surface principal strain, ε_{1a} , at the point of unloading.

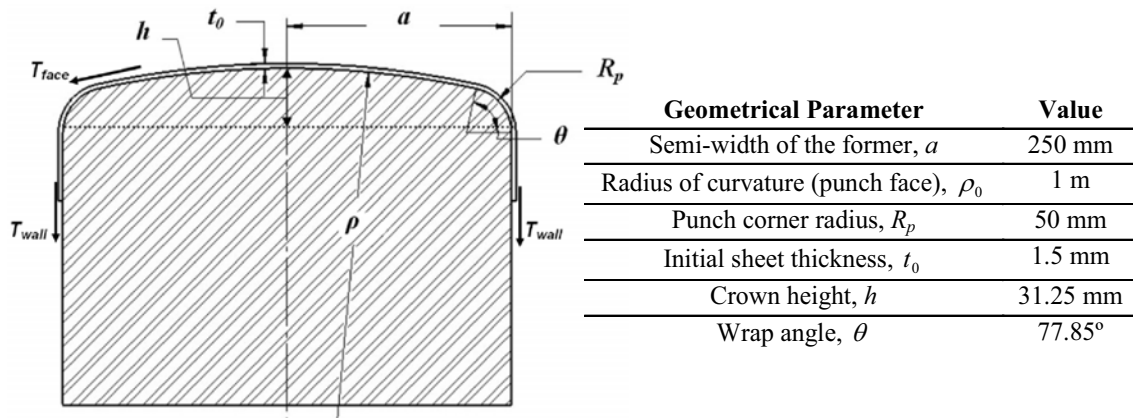


FIGURE 3. Two-dimensional stretch forming operation.

To assess the sensitivity of the sheet metal process to variation in input parameters, a multivariate probabilistic modelling approach was adopted. Probabilistic modelling is primarily based on the application of statistics for probability assessment of uncontrollable events. A multivariate probabilistic model permits the introduction of multiple noise parameters for analysis, where each noise parameter has a univariate normal distribution. For example, the variability in yield stress in an incoming coil is represented by a normal distribution of yield stress in individual blanks assessed from information in the literature on steel variability. We denote the n-dimensional joint-normal distribution with a mean vector \bar{x} and a covariance matrix ω , hence the probability density function is:

$$f(x_n | \bar{x}, \omega) = \frac{\exp\{-(1/2)(x - \bar{x})^T \omega^{-1} (x - \bar{x})\}}{\sqrt{(2\pi)^n |\omega|}} \quad (5)$$

A full-factorial DOE was performed for five noise parameters (yield stress, n-value, Young's Modulus, sheet thickness and friction co-efficient) at five equi-spaced levels to generate an appropriate output response space. For each DOE run, the probability of the inputs occurring was calculated using Equation (5) and, in turn, the likelihood of the output is determined. Springback histograms for various operating windows, assessed by analysing various sidewall tensions, are represented in Figure 4. The reject rate for each process setup state and, subsequently, its robustness can be assessed.

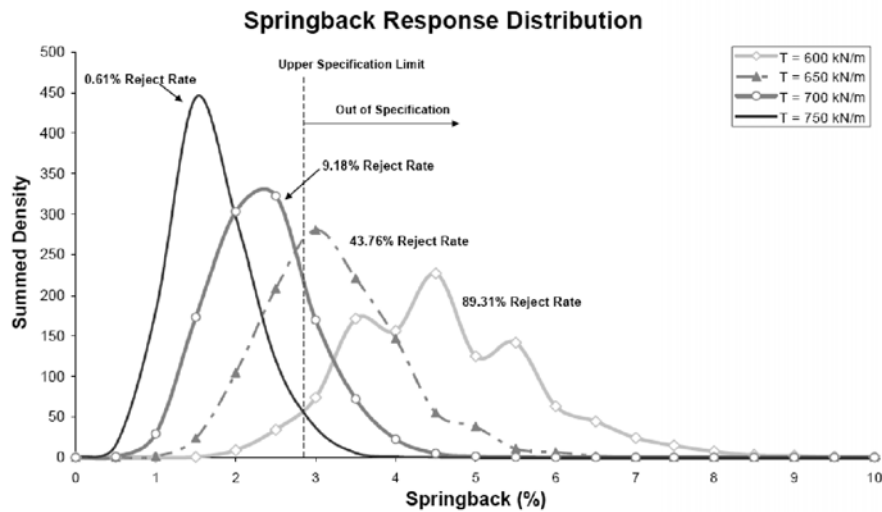


FIGURE 4. Springback distributions for a range of sidewall tensions and reject rate given an upper specification limit.

From Figure 4, it may be seen that for the variability parameters selected, the rejection rate is very sensitive to side-wall tension (indicative of binder pressure). For a tension of 600 kN/m the reject rate is 89%; this drops to less than 1% if the tension is increased to 750 kN/m.

Stochastic modelling is well suited to analytical modelling methods, primarily due to extremely short solution times compared to Monte Carlo finite element techniques which often involve running hundreds of individual simulations. Analytical models of this type could be used by manufacturers during initial feasibility and try-out stages to assess the 'true' performance of their stamping processes.

BENDING OF METAL/POLYMER LAMINATES

Material in which a thin polymeric sheet is sandwiched between two sheets of steel or aluminium has been used in the automotive industry and found to be effective in reducing weight and noise transmission. To improve the understanding of forming this sheet, a bending model was created [7]. It was assumed that the moment due to bending of the core would be negligible and the polymer was modelled as a material having a zero Young's Modulus, but a finite elastic shear modulus. In bending the sheet in a circular die, the outer sheet is stretched and the inner one is compressed (Figure 5a). Figure 5b shows a schematic illustration of the shear stress acting at the interface AB due to the shear deformation of the interlayer and the resulting tension in the outer cover sheet.

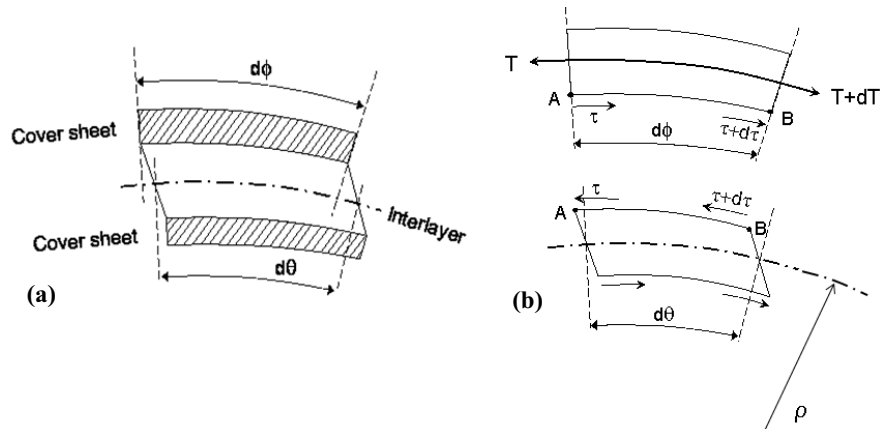


FIGURE 5. a) An element of the laminate material bent at a constant radius of curvature. b) Force equilibrium diagram of both the cover sheet and the interlayer.

The force equilibrium within the cover sheets was determined which led to:

$$T(\theta, \rho) = \frac{2aE'}{\rho} \left\{ (a + b) - b \frac{d\gamma}{d\theta} \right\} \quad (6)$$

With the tension force T , the shear angle θ , E' , the plane strain modulus, the radius of curvature ρ , half the thickness of the cover sheets and the interlayer a and b respectively and the rate of change of shear strain $\frac{d\gamma}{d\theta}$. (The shear modulus is included in determining the shear strain [7]). Assuming that the bending moment on the interlayer is small relative to the cover sheets and can be neglected, the bending moment on the laminate is composed of the moment to bend each cover sheet plus the moment due to the tensions on each cover sheet.

$$M_{total} = M_{upper} + M_{lower} + 2(a + b)T(\theta, \rho) \quad (7)$$

Equation (6) and (7) were applied to investigate the bending moment in a metal/polymer laminate that is bent to a circular arc in a frictionless die (Figure 6a).

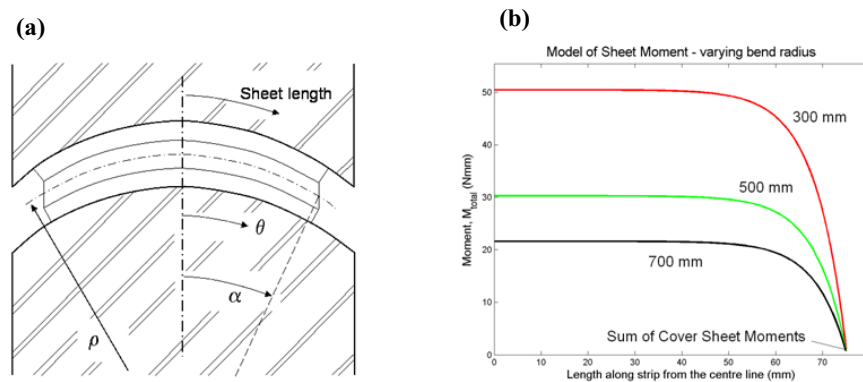


FIGURE 6. a) Bending of the metal/polymer laminate material to a constant radius of ρ for a frictionless clamped die. b) The moment diagram of the metal/polymer laminate bent to a circular arc for different values of the bend radius.

The results showed that the moment in the laminate is non-uniform along the bent strip (Figure 6b), even though the curvature is constant. This is due to tension and compression forces introduced in the cover sheets by the shear reaction force of the interlayer material. In a second approach [8] the model was extended to the elastic plane strain deformation of a strip that overhangs the die as shown in Figure 7.

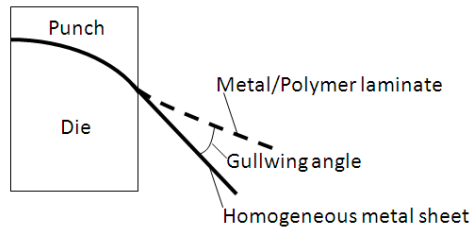


FIGURE 7. Schematic of a homogeneous metal strip and a metal/polymer/metal laminated sheet clamped between dies of circular profile showing the difference in the shape of the free standing strip (Gullwing defect).

The schematic diagram compares the free-standing shape of a homogeneous steel strip clamped between two dies of circular profile and that of the metal/polymer laminate. In both cases, the strip is tangent to the die surface at the edge and while the overhanging steel strip is straight, in the laminate there is a reversal of curvature at the tangent point (reverse bend). The model developed was applied to study the influence of process parameters on the shear deformation of the core, the tension forces within the cover sheets and the final shape of metal/polymer laminated strip. The investigation of the deformation of the free bending sheet outside the tooling showed that the reverse bend defect is due to tension within the cover sheets, which is a result of the core shear stress transferred at the interface between the core and the cover sheet layer. An additional benefit of the model is that it permitted the calculation of the stress at the interface; in practical forming operations, this stress can exceed the bond strength leading to delamination.

LOW PRESSURE TUBE HYDROFORMING (LPTH)

A new technology called low pressure tube hydroforming (LPTH) has gained increasing attention in the automotive industry for the forming of high strength steels. In this process a fluid filled and pressurized tube is formed to the required shape using a moving die (Figure 8) leading to a significant reduction of the internal pressure and die closing force required to form the part compared to the conventional hydroforming process. To improve the understanding of the process and to evaluate the die closing force and internal tube pressures needed to form a simple, wrinkle free part, a simplified analytical model was developed [9] for the low pressure tube hydroforming of a rectangular tube shown in Figure 8.

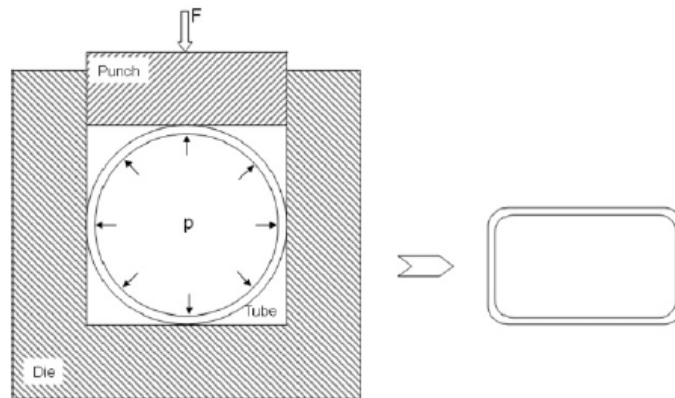


FIGURE 8. Schematic of low pressure hydroforming and the part shape analysed.

The model assumed a symmetrical deformation of the tube with negligible change in tube perimeter and a constant and uniform wall thickness. A rigid, perfect plastic material model was used and the tension in the tube wall was assumed constant around the corner radii. It was found that the die closing force consists of two major components: one is the compressive force in the tube wall to deform the corner radius and the other is the force due to the internal pressure that is transmitted through the tube wall contacting the upper die. The relation developed for the die closing force is given by.

$$F = 2p \cdot 1.165\Delta + 2T \quad (8)$$

With the internal tube pressure, p , the compressive force in the tube wall, T , and the displacement during forming, Δ . The model developed further showed that the circumferential compressive force in the tube wall required to form the material into the die corners increases as the corner radius decreases. The comparison with experimental and numerical results, Figure 9, showed sufficient agreement for initial process design.

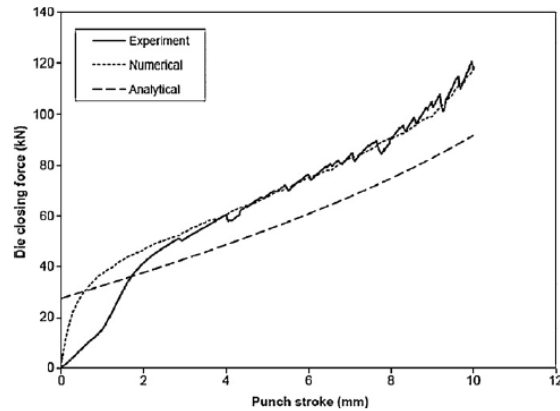


FIGURE 9. Die closing forces for the forming of a pressurized tube (10 MPa) at 10 mm die displacement.

INVERSE MODELLING

Researchers at Deakin University recently developed a free bending test for the investigation of the material behavior of metal strip at forming strains close to yield [10]. The test is of particular interest in studying the roll forming process where small changes in yield can lead to major forming defects. It was found that for some materials there is a significant difference between the elastic plastic transition in bending calculated from the yield point measured in the tensile test and that observed in actual bending; this was ascribed to residual stresses in the material introduced by manufacturing processes such as skin passing and roller leveling. It was concluded that for forming processes where bending is the major deformation mode, such as the roll forming process, material data based on the bending test may lead to improved accuracy in CAD and FEA based design packages [11, 12]. A typical moment curvature diagram obtained in the free bending test is shown in Figure 10a.

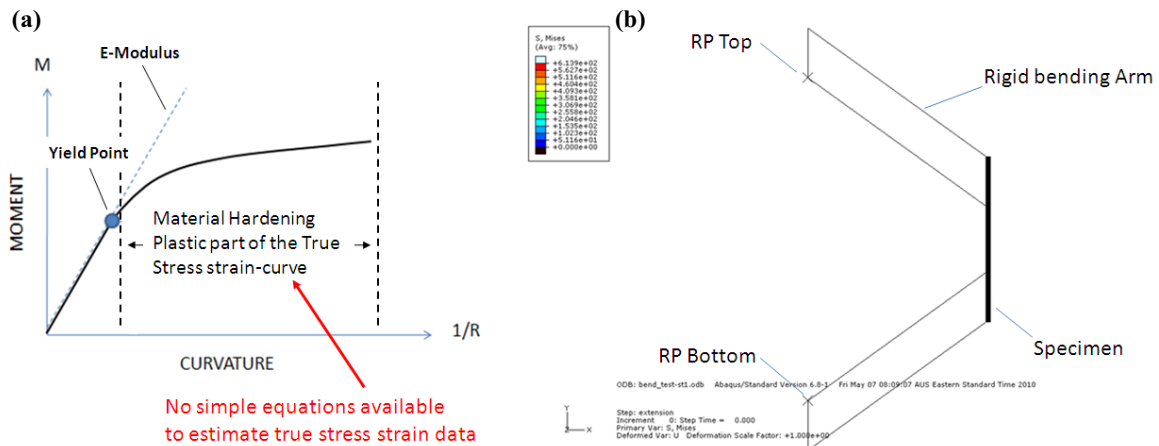


FIGURE 10. a) Moment curvature diagram determined in the pure bending test. b) Numerical model of the bending test.

While the Young's modulus and the bending yield stress can be determined by simple analysis of the elastic portion of the curve, a direct conversion of the moment curvature diagram in the elastic plastic region into a plastic true stress strain curve is not possible by a simple analysis. An inverse routine was therefore developed that is based on a numerical model of the bending test (Figure 10b); the output is a true stress strain law that if used in a simple bending model will reproduce the experimental moment curvature characteristic [13]. This is a simplification in that it neglects residual stresses in the material and other non-uniformities, but this is justified as many existing modeling packages for bending analyses also ignore these effects. Since the material properties for the elastic region (Yield Point and the Young's Modulus) are directly measurable from the bending test data the inverse routine is limited to the plastic region. The constitutive equation used here is:

$$\sigma = YP + \{H(\epsilon_p)\}^c, \text{ for } \sigma > YP \quad (9)$$

where the parameters H and c are the variables to be found. (H is the strength coefficient and c the plastic strain hardening index). A schematic of the inverse modelling system is shown in Figure 11.

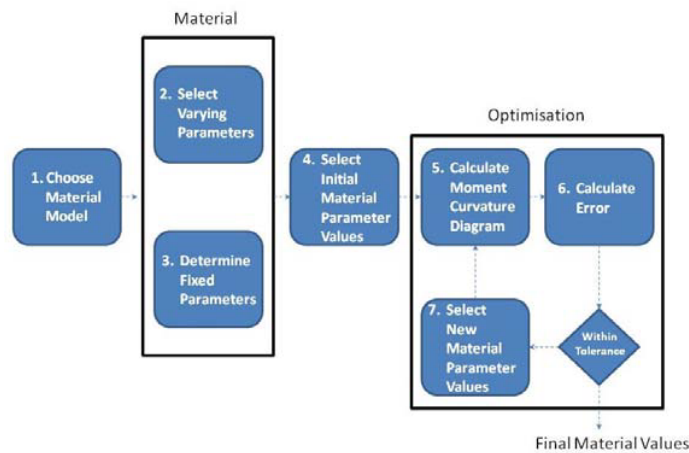


FIGURE 11. Schematic of the inverse model used showing the seven main steps.

At the start, an initial guess of the best values of tensile parameters is given to the optimization routine, (step 4) and a moment curvature diagram is numerically predicted using the FEA model of the bending test (step 5) and the estimated tensile curve. A root-mean-squared error is used to calculate the difference between the estimated and experimental moment-curvature curves (step 6) and an optimized set of material parameters (H and c) is found using a Matlab optimization command. Using the optimized tensile input, a second iteration (steps 4-7) is started; this process is repeated until the difference between the estimated and experimental moment-curvature characteristic is below a value set by the operator. The true stress strain curve generated can be used in numerical models of the roll forming process. Initial studies have indicated that for some conditions, improved model accuracy can be achieved if material input based on the bending test is used instead of conventional tensile data [14].

This method of obtaining a simple material law from the bending test is not a closed-form analysis, but it is included in this work as the outcome, i.e. the material equation, can be used for simple, approximate analyses of processes of the type given in other examples.

UNSTABLE BENDING OF SHEET

A technological defect in free bending of aged steel sheet is the formation of creases or kinks due to an instability in bending; it manifests as sharp bends across the width when uncoiling sheet and as creases in roll forming. It may also appear when bending a sheet over a die radius; instead of the sheet curving smoothly, facets appear that are separated by sharp bends. The phenomenon is, in some respects, analogous to the onset of diffuse necking in a tensile test. Diffuse necking starts when the load reaches a maximum allowing one portion of the test-piece to strain in an accelerated manner to failure, while material on either side unloads elastically. Similarly it may be postulated that in bending, the process will be stable if the moment curvature characteristic has a positive slope and unstable if

the slope is negative [15]. To study this, an analysis was required for the moment in free bending a strip having the stress strain characteristic shown in Figure 12; this shows that the elastic plastic transition occurs at an upper yield stress, σ_u , followed by deformation at a plastic flow stress, σ_f ; the degree of ageing can be represented by,

$$\lambda = \frac{\sigma_u}{\sigma_f} \quad (10)$$

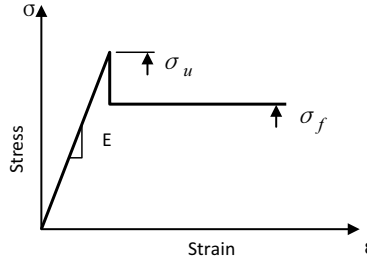


FIGURE 12. Assumed stress strain relation in aged sheet.

Assuming a linear strain distribution in bending, i.e. $\epsilon_b = \frac{y}{\rho}$, the stress distribution through the thickness is shown in Figure 13, where the elastic plastic transition is at a distance, $y_e = \rho \frac{\sigma_u}{E}$, from the mid-surface.

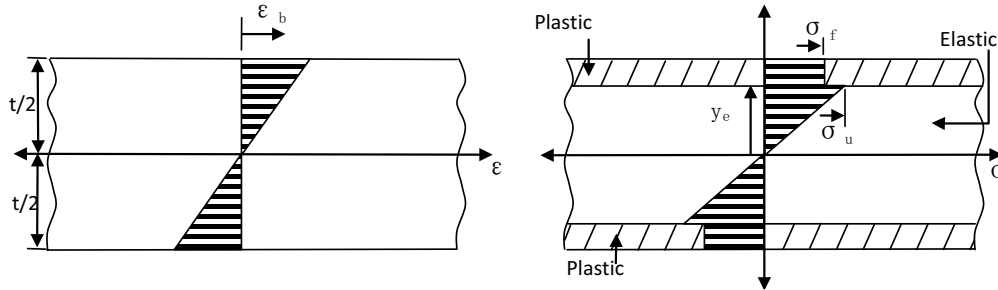


FIGURE 13. Assumed strain and stress distribution in bending of aged sheet.

The equilibrium equation for this stress distribution is [3],

$$M = 2 \int_0^{y_e} \frac{E}{\rho} y^2 dy + 2 \int_{y_e}^{t/2} \sigma_f y dy \quad (11)$$

where M is the moment per unit width. From this, we obtain,

$$M = \sigma_f \left\{ \frac{t^2}{4} + y_e^2 \left(\frac{2\lambda}{3} - 1 \right) \right\} \quad (12)$$

The moment curvature diagram calculated for different values of λ is shown in Figure 14. This is for a typical case of aged carbon steel in which, $t = 1 \text{ mm}$, Young's modulus $E = 200 \text{ GPa}$ and the flow stress is, $\sigma_f = 180 \text{ MPa}$. For no ageing, the upper yield stress, σ_u , is equal to the flow stress, i.e. $\lambda = 1$, and the curve has a positive slope throughout and stable bending is expected. For aged material with an upper yield stress of, $\sigma_u = 270 \text{ MPa}$, i.e. $\lambda = 1.5$, the slope of the curve is zero after yielding and this would be the start of unstable bending. For a heavily aged material with an upper yield stress of, $\sigma_u = 324 \text{ MPa}$, i.e. $\lambda = 1.8$, the slope of the curve beyond elastic bending is negative and the bending would be unstable. From this, it was proposed that the criterion for the onset of unstable bending or kinking is,

$$\lambda \geq 1.5 \quad (13)$$

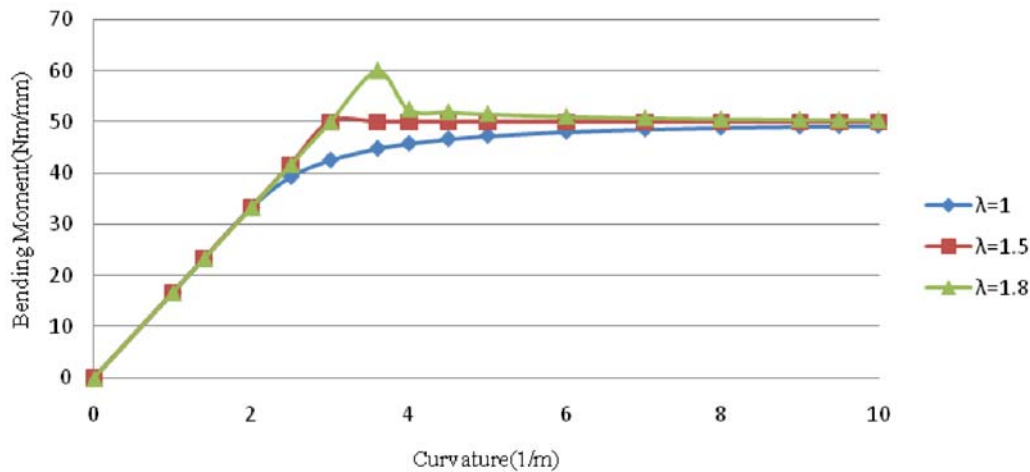


FIGURE 14. Theoretical moment–curvature diagram in bending aged materials without tension.

Experiment shows that if the upper yield stress is determined from a bending test rather than from a tensile test and the flow stress is obtained by back extrapolation of the true stress strain curve, this criterion is reasonable [15,16,17].

CONCLUSION

The approximate and simplified models presented have been useful in the initial study of a wide range of manufacturing processes, both for the initial assessment of the magnitude of variables in process design and also to assist students in understanding the factors governing common processes. They are not intended to replace more accurate numerical or analytical models, but rather to provide additional tools for industrial metal formers and for students entering this field.

ACKNOWLEDGMENTS

The authors thank those students whose work is included here, specifically Daniel Hurst, J Supasuthakul and Chetan Nikhare and also Emeritus Professor J L Duncan for his input.

REFERENCES

1. Bland, D. R., Ford, H., the calculation of roll force and torque in cold strip with tensions. Proc. Inst. Mech. Engrs 159, 144 (1948).
2. Gardiner, F., J. 'The spring back of metals', Tram. Am. SOC. mech. Engrs 1943 65,817.
3. Marciniak, Z., J.L. Duncan, and S.J. Hu, *Mechanics of Sheet Metal Forming*. 2nd ed. 2002: Butterworth-Heinemann. p. 211.
4. Supasuthakul, J., P.D. Hodgson, M. Weiss, and C. Yang, *Analytical Solutions and Finite Element Modelling of Deep Drawing Process for Cylindrical Metal Cups*. Key Engineering Materials, 2010. **443**: pp. 104-109.
5. Supasuthakul, J., *Modelling of Bending-Dominated Forming Processes of Metal Sheets*, PhD Thesis. Deakin University, Victoria. 2011.
6. de Souza, T. and B.F. Rolfe, *Multivariate Modelling of Variability in Sheet Metal Forming*. Journal of Materials Processing Technology, 2008. **203**(1-3): pp. 1-12.
7. M. Weiss, B.F. Rolfe, M. Dingle, J.L. Duncan, Elastic Bending of Steel-Polymer-Steel Laminates (SPS) to a Constant Curvature, Journal of Applied Mechanics (ASME), 2006. **73** (4): p. 574 - 579.
8. Weiss, M., An investigation on the forming behaviour of metal/polymer laminates, in Faculty of Science and Technology. 2006, Deakin University: Geelong. p. 214.
9. C. Nikhare, M. Weiss and P. D. Hodgson, Die closing force in low pressure tube hydroforming, Journal of Materials Processing Technology, 210 (2010) 2238-2244.
10. Weiss, M., et al., Measurement of bending properties in strip for roll forming, in International Deep Drawing Research Group, D.K.M. B.S. Levy, C.J. Van Tyne, Editor. 2009: Golden, Colorado, USA. p. 521-532.

11. Weiss, M., Y. Chunhui, and B.F. Rolfe, The effect of skin passing on Bending and Tension: An experimental Investigation, *Steel Research International*, 2010. 81(9): p. 789-792.
12. Weiss, M., et al. The effect of skin passing on the material behavior of metal strip in pure bending and tension in NUMIFORM 2010: Proceedings of the 10th International Conference on Numerical Methods in Industrial Forming Processes Dedicated to Professor O. C. Zienkiewicz (1921-2009). AIP Conference Proceedings. 2010. Pohang: American Institute of Physics
13. Weiss, M., B.F. Rolfe, and P.D. Hodgson, Comparison of bending and tensile properties for automotive grade strip steel, in *International Deep Drawing Research Group*. 2010: Graz, Austria.
14. Henning, R., et al., Understanding the shape defects in roll forming using a novel material characterising method, in *Symposium of Plasticity 2011*. 2011: The Casa Magna Marriott Puerto Vallarta Resort & Spa.
15. Ding, S.C. and J.L. Duncan, Instability in bending-under-tension of aged steel sheet. *International Journal of Mechanical Sciences*, 2004. 46(10): p. 1471-1480.
16. J. L. Duncan, M. Sue-Chu, X. J. Wang, Instability in plastic bending of thin sheet, in: C. J. (Ed.) *Mechanical behaviour of materials -IV*, Pergamon press: Stockholm, Sweden, 1993.
17. Weiss, M., et al., Effect of thermal treatment on the bending properties of pre-strained carbon steel. *Materials Science and Engineering: A*, 2011. 528(13-14): p. 4528-4536.